CHAPTER V

STRATOSPHERIC IMPLICATIONS AND FUTURE DIRECTION

5.1 INTRODUCTION

The experimental studies discussed in the last three chapters (Chapter II, III, and IV) describe some physico-chemical processes, which can generate mass independent isotopic fractionation in the product phases. These experiments were designed keeping in mind the processes taking place in the stratosphere, where mass independent signatures in some trace molecules have been discovered (e.g. stratospheric ozone, CO_2 etc.). For most of the cases, the sources of these mass independent isotopic signatures are still to be deciphered. The present study is expected to be useful in this regard. This study can also lead us to speculate about some other stratospheric molecules where mass independent signature is expected to be present. The present chapter will deal with these aspects in some detail.

5.2 STRATOSPHERIC IMPLICATIONS

The mean ozone concentration in the stratosphere is calculated by the Chapman function, which involves product of molecular oxygen concentration, UV flux and the photolysis cross-section. Figure 5.1 shows the depth of solar energy penetration through the atmosphere and Figure 5.2 shows the photon absorption cross-sections of oxygen and ozone molecules. These two together determine the ozone concentration profile shown in Figure 5.3. It has a nearly symmetrical shape with the maximum occurring at about 27 km altitude (Banks and Kockarts, 1973; Seinfeld and Pandis, 1998). As it is well known, this profile is not invariant in space and time and at a given region the observed profile represents a balance between constant production of ozone (from oxygen) and dissociation of ozone by UV. Just as ozone concentration profile is determined basically by the product of oxygen concentration, the UV flux at a particular altitude, and the cross-section, the ozone dissociation profile is determined by the product of ozone concentration (Figure 5.3), absorption cross-section (Figure 5.2) and the UV flux and is shown in Figure 5.4. As a consequence, the dissociation profile is similar to the concentration profile in shape but the maximum is shifted upwards in altitude (Banks and Kockarts, 1973) and occurs between 30 to 40 km in mid-latitudes.

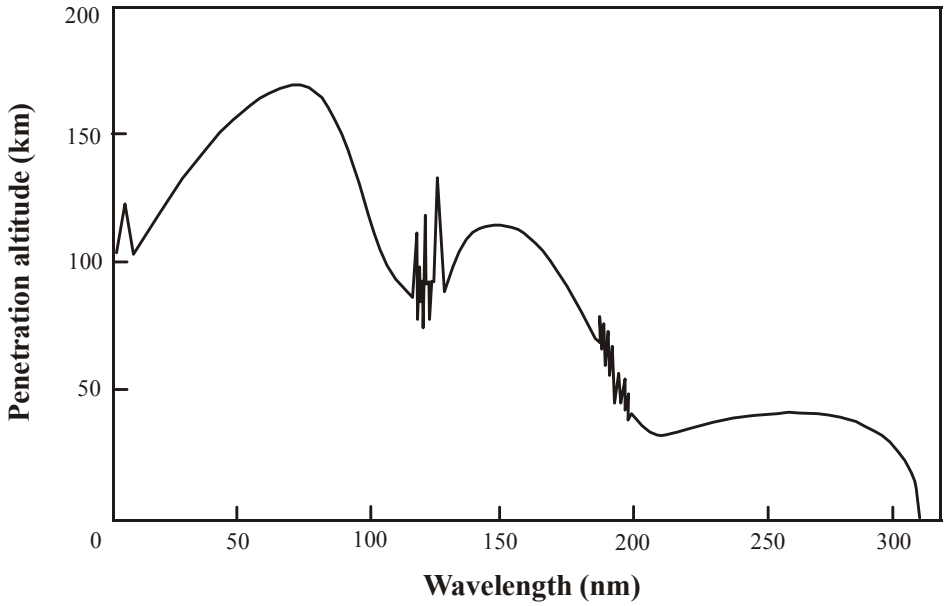

Figure 5.1. *Depth of penetration of solar radiation through the atmosphere. Penetration altitude corresponds to an attenuation of the incident radiation by a factor of e (reproduced from Seinfeld and Pandis, 1998).*

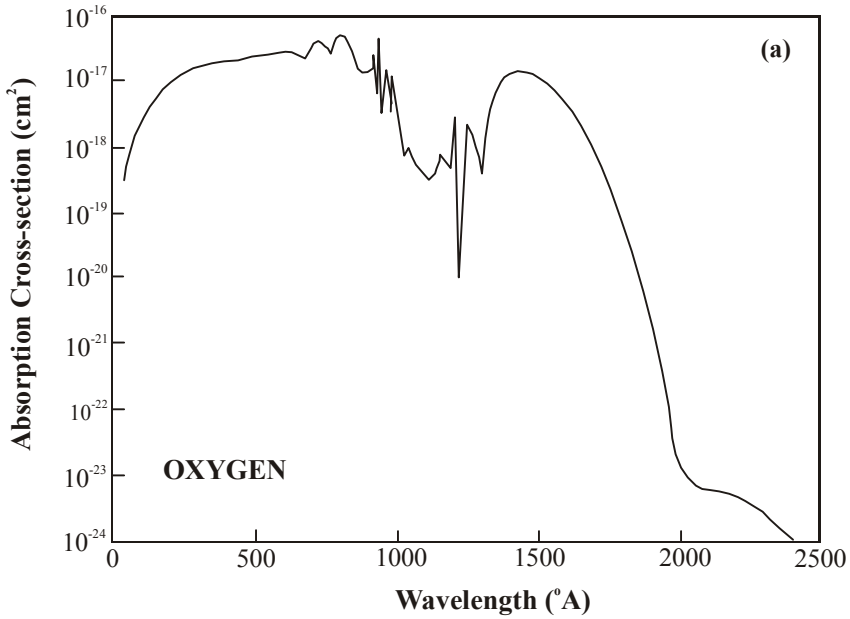

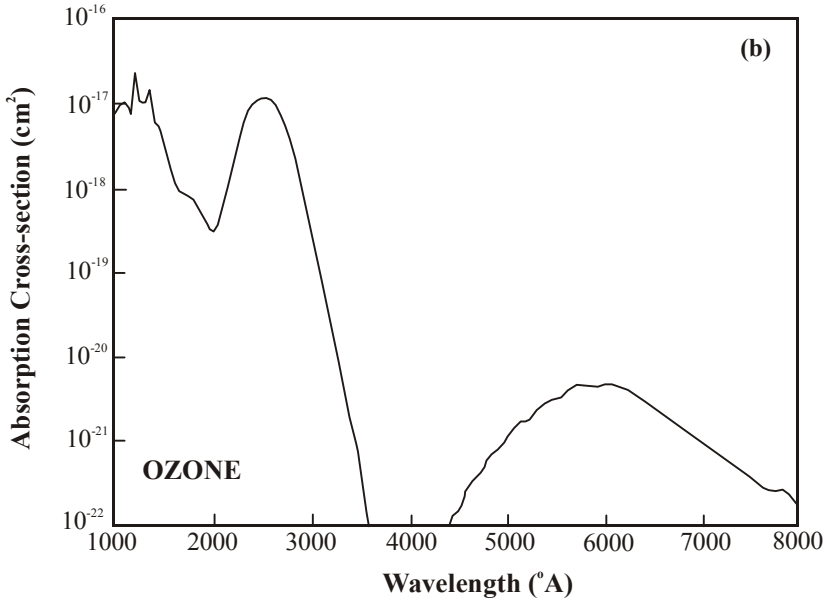

Figure 5.2. *Wavelength dependent absorption cross-section of (a) oxygen and (b) ozone molecule [reproduced from Yung and DeMore, 1999].*

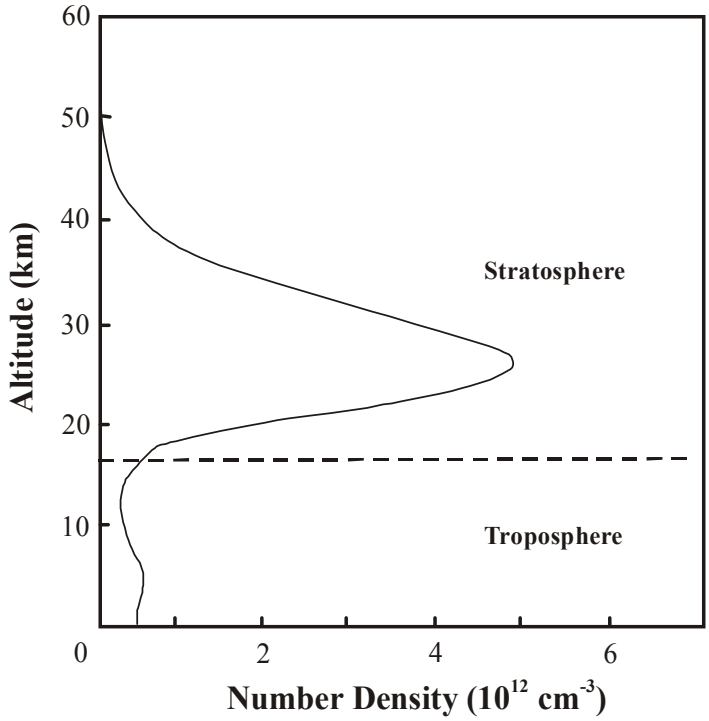

Figure 5.3. *Ozone molecular number density profile in the atmosphere showing a peak at an altitude of around 27 km. The corresponding concentration at the peak region is around 30 ppb. The concentration level goes down rapidly above and below this typical altitude, which varies depending upon latitude and season [reproduced from Seinfeld and Pandis, 1998].*

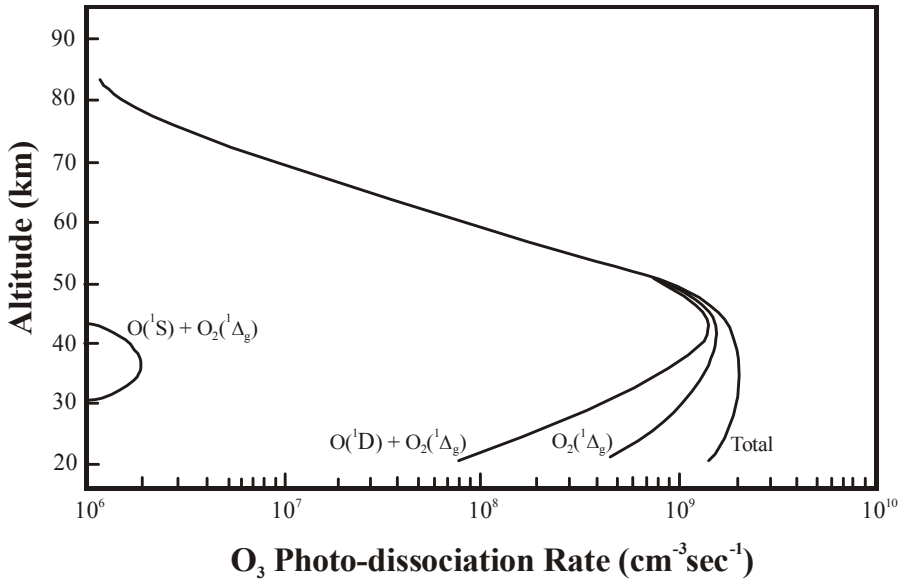

Figure 5.4. *Altitudinal variation of photo-dissociation rate of ozone in different state of O_2 and O [reproduced from Banks and Kockarts, 1973].*

5.2.1 Isotopic Enrichment Profile ($\Delta\delta^{18}O$) of Stratospheric Ozone

Though it is firmly established that the ozone in stratosphere is isotopically enriched, the nature of the variation of enrichment with altitude is not very clear. Since the ozone concentration is only about 30 ppb at the stratospheric peak (Figure 5.3), the isotopic measurements are difficult and have large uncertainties. Two types of techniques have been employed for this purpose: the mass-spectrometric methods and the spectroscopic methods (as described in Chapter I, § 1.4). The mass-spectrometric methods are presumably more accurate but initially the data were beset with unknown sources of error. Recent summary by Mauersberger et al. (2001) made a critical review of earlier measurements and showed that isotopic enrichment increases with altitude, initially slowly but sharply above about 30 km as shown in Figure 5.5 (the highest enrichment that was considered acceptable is about 110 ‰ at 33 km). Irion et al. (1996) reported integrated enrichment in $^{50}O_3$ of 130 ‰ (with large error of 50 ‰) between 25 to 41 km based on ATMOS Infrared solar spectra. Meier and Notholt (1996) reported a similar level of enrichment with smaller error. Since the average itself is 130 ‰, it is expected that much higher level of enrichment would prevail at altitudes beyond 30 km taking mass-spectrometric values (Mauersberger et al., 2001) at the lower level as representative. The high values beyond 30 km are also supported by the studies of Goldman et al. (1989) and Abbas et al. (1987). The former showed column-averaged

isotope enhancement (all in ‰) above 37 km to be 330 ± 160 and 220 ± 100 ‰ while the latter showed enrichment of 180 ± 140 ‰ at 25 km and 450 ± 140 ‰ at 37 km.

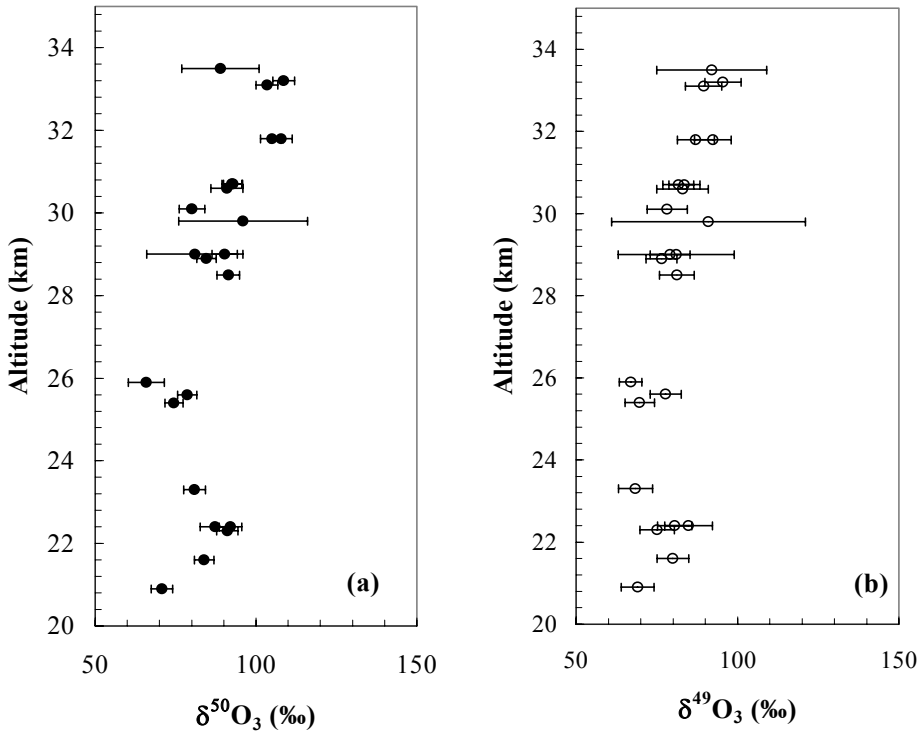

Figure 5.5. *Compiled data of altitudinal variation of stratospheric ozone enrichment (a) enrichment in ^{18}O (≡$^{50}O_3$) and (b) enrichment in ^{17}O (≡$^{49}O_3$) [data from Mauersberger et al., 2001].*

5.2.2 Altitudinal Variation: Previous Explanation and Present Proposition

Mauersberger et al. (2001) attempted to explain the altitude variations in ozone isotopic enrichments through temperature dependence. In stratosphere, as one goes up the temperature increases, from about 217.6 K at 21 km to about 231 K at 33 km. It was surmised that since the enrichment increases with increase in temperature, as observed by Morton et al. (1990), the stratospheric temperature increase can account for the altitude variation. However, there are some difficulties in accepting this explanation with temperature as the sole cause of observed increase, especially the high variability. The temperature coefficient determined by Morton et al. (1990) pertains to ozone recycling experiment using visible light as the dissociating agent (in the Chappuis band of 500 to 700 nm), which is not the major agent of dissociation in the stratosphere. It is also noted that the experimental data points show large scatter (Figure 3 from Morton et al., 1990) through which it is difficult to fit a well-defined line. Even if one neglects these points,

the total temperature change from 21 km to 33 km is only 13.4 K and assuming an average temperature coefficient (0.6 ‰ per K) from Morton et al. paper one would expect an increase of only about 8 ‰ which is far too small compared to the observed increase of about 30 ‰. The problem is more serious when one considers other spectroscopic data showing very high enrichments at high altitudes. Based on these considerations it is clear that temperature dependence can only account for a small part of the total increase in stratosphere.

On the contrary, the experimental results obtained in the present study (Chapter II) show that significant enrichments could be obtained in the laboratory if formation and dissociation are allowed to proceed within a certain pressure range where the turn-over time ($\tau = [O_3] / d[O_3]/dt$, where $[O_3]$ is the ozone amount at a given time and $d[O_3]/dt$ is the dissociation rate at that time) of the ozone reservoir is short (Chapter II, § 2.4.4; Bhattacharya et al., 2002). The stratospheric situation is, of course, not exactly similar to that of the experiment described in Chapter II, but the basic process regulating the enhancement of fractionation should be similar. Two major differences between stratosphere and laboratory experiments are readily apparent – presence of four times abundant nitrogen (helping in collisional deactivation of ozone complex) and the absence of a confining surface. Theis would result in higher relative production and increase the value of τ.

Figure 5.5 shows the variation of ozone isotopic enrichment with altitude in stratosphere as summarized by Mauersberger et al. (2001) and shows a fitted line to the data. It also shows the calculated turn-over time with pressure (or altitude) for stratospheric ozone (estimated using the data of Banks and Kockarts (1973) of ozone concentration and dissociation rate in the stratosphere as shown in Figures 5.3 and 5.4). For comparison, PRL config I profile (Chapter II, Figure 2.4) is given against the oxygen pressure. Lower limit estimates of τ for the PRL config I data in the peak zone are also indicated alongside the enrichment profile. To compare the stratospheric enrichment profile with the laboratory profile, we have to first correct the laboratory data for the temperature effect. The experiments were done at room temperature, at about 300 K, whereas the mean stratospheric temperature at 25 km is about 225 K. Assuming an increase of 0.6 ‰ per K increase we have to subtract about 45 ‰ from the laboratory data. It is interesting to note that, after this correction, the variation of enrichment with

pressure shows a similar trend as observed in the stratosphere and the values are also in the same range.

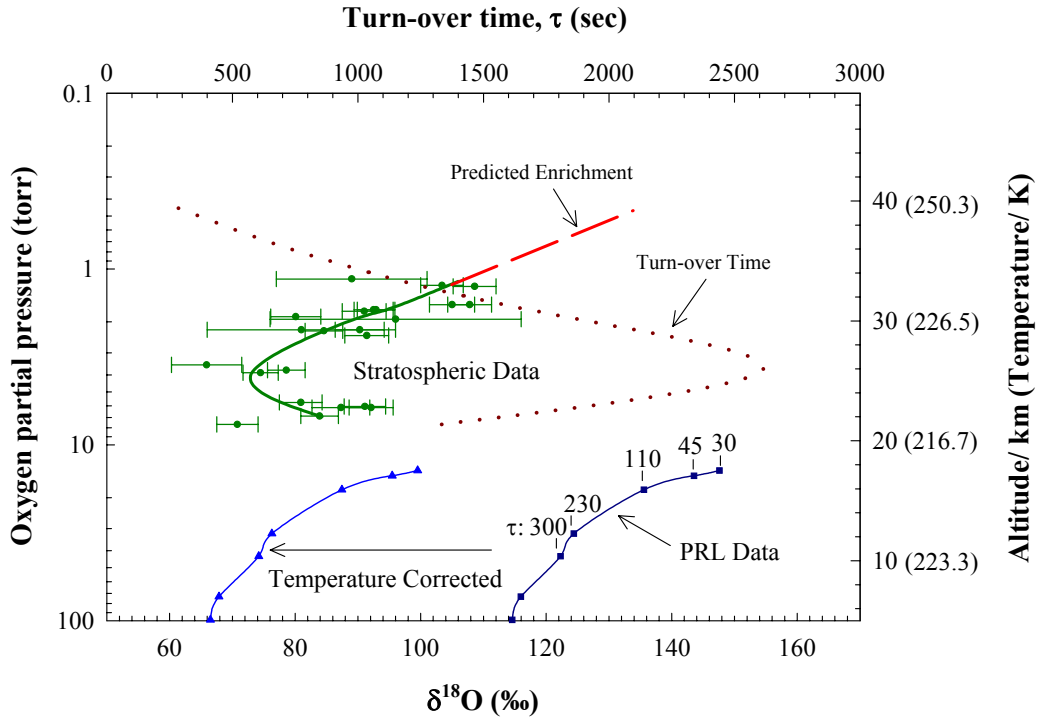

Figure 5.6. *Comparison of variation of isotopic enrichment ($\delta^{18}O$) as observed in the stratosphere and in the laboratory. The trend in enrichment variation with altitude (a fitted curve based on data from Mauersberger et al., 2001) and the variation of enrichment with pressure as obtained from the PRL experiment are shown. To compare the laboratory data with stratospheric data, the PRL profile has been corrected for lower stratospheric temperature. The PRL profile has τ values (which are approximate estimates) marked alongside. The variation of turn-over time τ as a function of altitude for stratosphere ozone is shown by the dotted line (upper scale). Note the inverse relation of τ with ozone isotopic enrichment in stratosphere allowing us to predict an enrichment variation with altitude beyond 33 km as shown (see text for explanation).*

It should be mentioned here that it is difficult to calculate the turn-over time for the laboratory data points since the experiments were not designed to get steady state concentration or isotope ratios. During the photolysis time, the ozone builds up and dissociates simultaneously; therefore, the turn-over time varies systematically. Taking the end point when the photolysis is terminated we can only get a lower limit of turn-over time. These values are shown in Figure 5.6 and vary from about 300 to 30 sec in the peak region. It is seen that the enrichment increases with decrease in the turn-over time as expected. The turn-over time for stratospheric ozone based on Chapman model (Banks and Kockarts, 1973) range from about 2550 to 1250 sec in the height range of 20 to 33 km. These are much higher than the laboratory values indicating slower recycling in the

stratosphere. An important reason for the difference in the τ values is the wavelength used for the laboratory experiment. Since the Hg lamp has emission peak at 253.7 nm, which happens to be near the peak in absorption of ozone the dissociation is very effective in case of laboratory experiments. Whereas, in case of stratosphere the solar actinic flux has very different structure and is altitude dependent. Notwithstanding this complexity, the turn-over time variation with altitude seems to be reverse of the enrichment variation based on a smooth fitting of Mauersberger et al. (2001) data. The reverse pattern is consistent with the expected turn-over time dependence as predicted from the experimental data (PRL data). Since the turn-over time decreases further with height, we expect further enrichment in isotopic ratio with altitude, which is consistent with values based on the spectroscopic methods mentioned before.

5.2.3 Application of Altitudinal Variation of Isotopic Enrichment in ^{18}O

The intimate relation of ozone isotopic composition and its dissociation in the stratosphere can have an interesting application. Since, absorption of UV by ozone and its dissociation is the major contributor for stratospheric heating, the altitudinal variation in isotopic enrichment of ozone could be used to monitor the heating rate variation. Only indirect methods are available so far for estimating this important parameter.

5.2.4 Altitudinal Variation in Slope of $\Delta\delta^{17}O - \Delta\delta^{18}O$ Correlation Plot

It is well known that dissociation of ozone is an important and continuous process in the stratosphere and both formation and dissociation play their role in determining the ozone concentration variation with altitude. It is also known that stratospheric ozone is enriched in heavy oxygen isotopes and the enrichment increases with altitude (§ 5.2.1). The proposition described in § 5.2.2 explains the altitudinal variation of $\delta^{18}O$, but does not consider the relative change between $\delta^{17}O$ and $\delta^{18}O$. Since numerous laboratory experiments have established that formation of ozone by UV photolysis of oxygen is associated with large mass-independent heavy isotope enrichment, stratospheric results are sought to be explained through formation process alone. But in view of the present experiments (Chapter II and III), which clearly show that photo-dissociation acts preferentially on the lighter isotopes and enriches the left-over ozone pool, it is pertinent to inquire about its role in modifying the ozone isotope ratios in the stratosphere.

The dissociation experiment (described in Chapter III) shows that photo-dissociation consists of two channels, i.e., pure photo-dissociation and $O(^1D)$ (ozone

derived) mediated dissociation and these two channels produce different isotopic effects. Both the dissociation channels enrich the left-over ozone pool, but the former does not distinguish between ^{17}O and ^{18}O, whereas the latter discriminates them in a mass dependent way. These two effects together result in a slope of 0.63 in photo-dissociation.

In the lower stratosphere, ozone formation is relatively more important than photo-dissociation but with altitude photo-dissociation becomes more and more important resulting in reduction of ozone concentration. The process of ozone formation results in an ozone reservoir where both the heavy oxygen isotopes (^{17}O and ^{18}O) are equally enriched (Thiemens and Jackson, 1987, 1988). In photo-dissociation of ozone in the stratosphere, the first channel (i.e., the photon-induced dissociation) is mainly responsible for the dissociation since the product $O(^1D)$ is quenched rapidly by N_2 and O_2. Since this results in equal enrichment of the two heavy isotopes, it follows that the relative enrichment would still be the same for ^{17}O and ^{18}O in the stratosphere (i.e., the two delta variations would have a slope value of unity). However, the observed stratospheric slope (up to ~ 35 km) is 0.62 (Lämmerzahl et al., 2002), a value well below unity. The deviation of the observed stratospheric slope from the expected value is puzzling and needs further scrutiny. It is, of course, clear that the stratospheric processes are not so simple as described above. Oxygen isotopic exchange between ozone and CO_2 (via ozone dissociation product $O(^1D)$) may have a role in controlling the isotopic composition of the ozone reservoir and will be discussed later. Additionally, there are other dissociation processes besides the photo-dissociation, which are similar to simple chemical reactions and probably result in mass dependent fractionations. The net effect of these would be to reduce the slope value from unity.

5.3 OXYGEN ISOTOPIC COMPOSITION OF STRATOSPHERIC CO_2

The oxygen isotopic composition of tropospheric CO_2 is controlled by the oceans and the land biota. On a global scale, isotopic exchange with vegetation and respiration processes produce an isotopic enrichment in ^{18}O, while exchange with soils acts to decrease the ^{18}O content (Ciais et al., 1997). The mean $\delta^{18}O$ of tropospheric CO_2 is enriched by ~ 41.5 ‰ relative to oxygen isotopic composition of ocean water (i.e. SMOW), with an annual average difference of ~ 2 ‰ between the two poles (Trolier et al., 1996).

The oxygen isotopic measurement ($\delta^{18}O$) of stratospheric (from 19 to 25 km) CO_2 was first carried out by Gamo et al., (1989) over Japan (39°N, 142°E). They found that at 19 km $\delta^{18}O$ of CO_2 was enriched by ~ 2 ‰ relative to the tropospheric value and the enrichment increased with increasing altitude. In a later publication (Gamo et al., 1995) they showed that the enrichment increased up to 7 ‰ at 35 km. A new dimension was added to this subject with the simultaneous determination of $\delta^{18}O$ and $\delta^{17}O$ in stratospheric CO_2 (Thiemens et al., 1991, 1995). The samples collected over Palestine, Texas (32°N, 96°W), and Fort Sumner, New Mexico (34°N, 104°W), at altitude between 26 to 35.5 km (Thiemens et al., 1991) were enriched by 7.9 to 12.6 ‰ and 10.0 to 15.5 ‰ in $\delta^{18}O$ and $\delta^{17}O$ respectively compared to the tropospheric level. These samples bear a mass independent signature expressed as $\Delta^{17}O$ (= $\delta^{17}O$ - 0.52 * $\delta^{18}O$) ranging from 5.2 to 9.5 ‰. The CO_2 collected over White Sands, New Mexico (32°N, 106.3°W) at altitudes between 29.3 to 60 km, showed higher enrichment of 4.1 to 14.5 ‰ with concomitant $\Delta^{17}O$ values ranging from 5.25 to 11.95 ‰ (Thiemens et al., 1995).

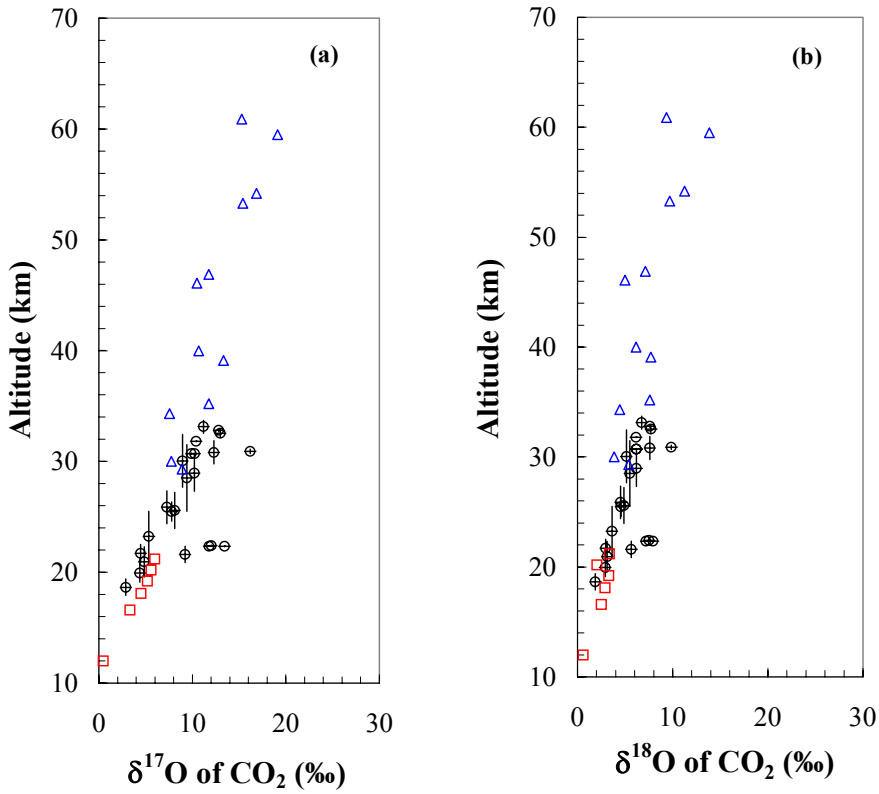

Figure 5.7. *Compiled data of altitudinal variation in oxygen isotopic enrichment (wrt tropospheric composition) in stratospheric CO_2; (a) enrichment in $^{17}O/^{16}O$ and (b) enrichment in $^{18}O/^{16}O$. Circles are the data from* Lämmerzahl et al., 2002, squares are from *Alexander et al., 2001 and triangles are from Thiemens et al., 1995. The observations clearly show the altitudinal variation of enrichment in ^{17}O and ^{18}O.*

The most recent stratospheric measurements by Lämmerzahl et al. (2002) over northern Europe at altitudes between 10 to 35 km demonstrate enrichment values up to 11 ‰ in $\delta^{18}O$ and 19 ‰ in $\delta^{17}O$. The stratospheric CO_2 data from the above papers are compiled in Figure 5.7. Figure 5.8 shows a covariation plot of $\delta^{17}O$ and $\delta^{18}O$ in stratospheric CO_2.

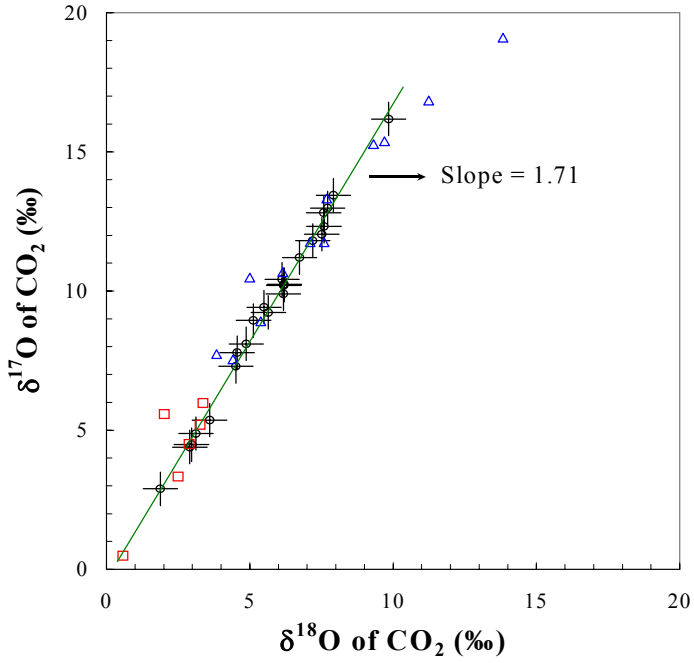

Figure 5.8. *Three-isotope plot of compiled data showing the variation in $^{17}O/^{16}O$ enrichment against $^{18}O/^{16}O$ enrichment (w.r.t tropospheric composition) in stratospheric CO_2. The circles are the data from Lämmerzahl et al., 2002, squares are from Alexander et al., 2001 and triangles are from Thiemens et al., 1995. A strong correlation between the $\delta^{18}O$ and $\delta^{17}O$ exist with a slope 1.71 for the enrichment up to 11 ‰ in $\delta^{18}O$ (for the data from Lämmerzahl et al., 2002). In the higher altitude where the enrichment is more than 11 ‰ (in $\delta^{18}O$) the same relationship does not hold; rather a lower slope (1.2) is observed.*

5.4 ROLE OF O(^{1}D) IN THE STRATOSPHERE

Photochemistry is the main driving force behind most of the reactions of the stratosphere. It initiates a large number of chemical cycles; the ozone cycle is one of the well-known examples. The O(^{1}D) is the most active photochemical product in the stratosphere. Depending upon the solar wavelength penetration (Figure 5.1) in the stratosphere, production of O(^{1}D) by the photolysis of O_2, O_3, NO_2, CO_2, N_2O is energetically possible (Okabe, 1978). Among these molecules, O_3 photolysis is the major source of O(^{1}D). Since the production of O(^{1}D) by photolysis of different oxygen

containing molecules in the stratosphere is ceaseless during the day, a certain level of $O(^1D)$ is present throughout the stratosphere (the concentration profile of $O(^1D)$, similar to that of ozone photo-dissociation rate profile with a maximum at around 40 km) in the day time. After sunset (after ~ 100 sec) all the oxygen atoms in the stratosphere disappear since there is no photo-dissociation of ozone or other molecules (Banks and Kockarts, 1973).

As an important part of atmospheric transport, the tropospheric air enters the stratosphere predominantly at the topical tropopause and is then dispersed slowly upward and towards the poles (Volk et al., 1996). During this transport air molecules act as quencher for the stratospheric $O(^1D)$ (Tully, 1975).

The electronic energy of $O(^1D)$ is 1.967 eV above the ground state. Since transition to the ground state $O(^3P)$ is forbidden by spin conservation (Okabe, 1978), the fate of this singlet atomic species is physical and chemical quenching. The chemical quenching of this active species governs a number of chemical reactions in the atmosphere (as for example, reactions with H_2O, N_2O etc.) (Tully, 1975). The physical quenching, especially with oxygen containing molecular species, is of great interest. At the time of quenching, the $O(^1D)$ can take part in an isotopic exchange with the oxygen atom of that molecule.

5.4.1 Isotopic Composition of $O(^1D)$

The isotopic composition of the $O(^1D)$ derived from ozone photo-dissociation is not known. Previous studies (Barth and Zahn, 1997; Yung et al., 1991, 1997) assumed negligible fractionation during the O_3 photolysis reaction. Consequently, the isotopic composition of the $O(^1D)$ reservoir was thought to be equal to that of the ozone reservoir. However, the present study shows that pure photo-dissociation of ozone (Chapter III) enriches the left-over ozone pool in a mass independent way with an instantaneous fractionation factor of about 7 ‰. The model calculations of Johnston et al. (2000) also show slightly enriched $O(^1D)$ reservoir. Moreover, it is now known that isotopic enrichment in ozone occurs primarily in the asymmetric isotopomers of ozone. The kinetic studies of Janssen et al. (1999) show a rate coefficient advantage in the formation channel of the asymmetric ozone molecule ($^{16}O^{16}O^{18}O$). Since during photo-dissociation of ozone the product $O(^1D)$ is likely to be derived from the terminal atoms, it should have an enrichment similar to that of asymmetric ozone molecules.

Janssen et al. (2001) calculated an enrichment of 129 ‰ in $^{50}O_3$ using the relative rate coefficient of formation by different channels (given in Table 1.1, Chapter I). Following the definition of enrichment (Janssen et al., 2001), i.e., E (‰) = [($^{M}O_3$/ $^{48}O_3$) $_{measured}$ / ($^{M}O_3$/ $^{48}O_3$) $_{calculated}$ −1] × 1000 ‰, and the rate constant of different ozone forming channels, the isotopic composition of the asymmetric ozone can be computed in the following way.

When oxygen and ozone molecules are formed from an isotopically scrambled O_2 molecule reservoir with atomic isotopic ratio f = $^{18}O/^{16}O$, we have by definition (statistically), 2f = [$^{18}O^{16}O$] / [$^{16}O^{16}O$] and 3f = [$^{18}O^{16}O^{16}O$ + $^{16}O^{18}O^{16}O$] / [$^{16}O^{16}O^{16}O$] for the ratios of $^{34}O_2$/ $^{32}O_2$ and $^{50}O_3$/ $^{48}O_3$. For atomic oxygen the ratio of ^{18}O/ ^{16}O is given by [^{18}O] / [^{16}O] = 0.924f, where atomic oxygen is in isotopic equilibrium with molecular oxygen. Using these definitions, the enrichment in asymmetric ozone can be expressed (in per mil) as,

$1 + E(^{50}O_3)^{asy} / 1000 = [\{k_{12}[^{18}O][\ ^{16}O^{16}O] / k_1[^{16}O][\ ^{16}O^{16}O]\} + \{1/2\ k_{10}[^{16}O][\ ^{16}O^{18}O] / k_1[^{16}O][^{16}O^{16}O]\}] / 2f$

where, k_1, k_{10} and k_{12} are relative rate coefficient of channels 1 ($^{16}O + {}^{16}O^{16}O \rightarrow {}^{16}O^{16}O^{16}O$), 10 ($^{16}O + {}^{16}O^{18}O \rightarrow {}^{16}O^{16}O^{18}O$) and 12 ($^{18}O + {}^{16}O^{16}O \rightarrow {}^{18}O^{16}O^{16}O$) given in Table 1.1 (Chapter I) (In the denominator, $(^{M}O_3/\ ^{48}O_3)_{calculated}$ is substituted by 2f since the asymmetric ozone species are only considered). Therefore, inserting the relative rate coefficient of channels 10 and 12 (1.45 and 0.95 respectively), we obtain, $E(^{50}O_3)^{asy}$ = 150 ‰.

Unfortunately, there are limited studies regarding the distribution of ^{17}O within the ozone isotopomers. Except channel 4 ($^{17}O + {}^{16}O^{16}O \rightarrow {}^{17}O^{16}O^{16}O$), the rate coefficients for the channels forming $^{49}O_3$ are not known. To calculate the enrichment of asymmetric $^{49}O_3$, the knowledge of rate coefficient of channel 2 ($^{16}O + {}^{16}O^{17}O \rightarrow {}^{16}O^{16}O^{17}O$) is specially required since similar kind of reaction channel (channel 10) forming asymmetric $^{50}O_3$ shows very high relative rate. Considering a zero point energy difference of 11.6 cm^{-1} between $^{16}O^{16}O$ and $^{16}O^{17}O$ (i.e. the isotopic exchange reaction corresponding to channel 2) and using the Δ(ZPE) vs. relative rate coefficient plot (Figure 1 of Janssen et al., 2001), a relative rate coefficient of 1.35 is obtained for channel 2. Following the steps similar to the calculation of $E(^{50}O_3)^{asy}$, we finally obtain, $E(^{49}O_3)^{asy}$ = 150 ‰. Therefore, under the terminal atom source assumption $O(^1D)$ has an enriched composition ($\delta^{17}O$ = 150 ‰ and $\delta^{18}O$ = 150 ‰) relative to the total initial oxygen. For our experiment the

oxygen has the composition of $\delta^{17}O$ = 12.48 ‰ and $\delta^{18}O$ = 24.58 ‰ with respect to SMOW. Therefore, $O(^1D)$ will have the composition, $\delta^{17}O$ = 164.1 ‰ and $\delta^{18}O$ = 178.3 ‰ with respect to SMOW.

5.4.2 Interaction of $O(^1D)$ With Other Oxygen Bearing Molecules

The physical quenching of $O(^1D)$ with oxygen bearing trace molecules result in isotopic exchange which alters the isotopic composition of those molecules. The alteration of isotopic composition of a molecule depends upon the nature of the exchange and in principle can take place in two different ways, (i) simple mixing of the two exchanging components and, (ii) isotope selective exchange.

The isotopic composition of CO_2 after isotopic exchange with $O(^1D)$ can not be interpreted by a simple mixing of CO_2 and $O(^1D)$ (as described in Chapter IV). An isotope selective exchange mechanism was hypothesized to explain the laboratory data, which reflects a slope ($\Delta\delta^{17}O/\Delta\delta^{18}O$) of about 1.8 in the exchanged CO_2, using the isotopic compositions of O_3 (the source of $O(^1D)$) and CO_2 similar to the atmospheric values. This slope is close to the value obtained recently in the stratospheric CO_2 (Lämmerzahl et al., 2002).

Even for the cases where simple mixing mechanism is operative during the isotopic exchange between $O(^1D)$ and a oxygen bearing molecule, a mass independent isotopic composition can be seen in the exchanged molecule if the $O(^1D)$ is derived from ozone since it bears mass independent signature.

Similar to the case of stratospheric CO_2 which inherits a mass independent signature due to the isotope selective exchange with $O(^1D)$, stratospheric CO is another potential candidate to look for a similar kind of effect since it has a similar quenching rate constant (7×10^{-11} cm^3/molecule-sec) as that of $O(^1D) - CO_2$ reaction (Heidner et al., 1972). Unfortunately, due to its very low stratospheric concentration (< 0.1 ppbv), it is difficult to investigate with present day facilities. However, these types of exchange reactions can be studied in the laboratory for better understanding of the transfer mechanism.

5.4.3 Importance of $CO_2 - O(^1D)$ Exchange

There are three significant oxygen reservoirs in the stratosphere. The major one is of course, the ambient oxygen. The other two are ozone and stratospheric CO_2. Two types

of oxygen atoms, i.e. $O(^3P)$ and $O(^1D)$ are the transient species and work as mediators between these three oxygen reservoirs. With increasing altitude, oxygen isotopic enrichment in both CO_2 and ozone increases progressively in stratosphere (Lämmerzahl et al., 2002) and the observed enrichment pattern relating $\delta^{17}O$ and $\delta^{18}O$ has slope values of 1.71 and 0.62 respectively. It is puzzling to see that the slope relating ozone isotopic enrichments is 0.62 despite the fact that both formation and photo-dissociation processes generate a slope of unity in laboratory studies. It is established from the present study as well as the earlier ones that the isotopic exchange between ozone and CO_2 via $O(^1D)$, transfers ^{17}O preferentially. This can make the stratospheric ozone pool relatively depleted in ^{17}O and result in a lower value of the slope.

The enrichment pattern found in set II data described in Chapter IV for CO_2 and initial ozone is of relevance at this point. Though the initial CO_2 composition ($\delta^{17}O$ = 8.98 ‰ and $\delta^{18}O$ = 17.28 ‰) and the variation in initial ozone composition (124.9 to 205.7 ‰ in $\delta^{18}O$) in the laboratory experiment are not representative of the stratospheric values (the isotopic composition of stratospheric ozone varies only by about 30 ‰ in $\delta^{18}O$), the relationship between the two slope values are quite similar and suggest intimate connection between these two interacting oxygen reservoirs.

In addition to the above exchange process, there are other processes influencing the ozone isotopic composition like catalytic ozone destruction cycles (namely by HO_X, NO_X, ClO_X cycles). The classical Chapman ozone cycle does not consider these destruction channels and thus predicts a higher ozone concentration (Seinfeld and Pandis, 1998). These destruction cycles are chemical processes and probably enrich the ozone reservoir in a mass dependent way since kinetic chemical reactions, in general, destroy lighter isotopes preferentially. Therefore, the exchange process with CO_2 and these destructive ozone cycles together can influence the relative enrichment between ^{17}O and ^{18}O in the stratospheric ozone to produce a net slope of 0.62.

5.5 FUTURE LABORATORY STUDIES

There are several exchange reactions, which can impart the mass independent signature of ozone to other oxygen containing atmospheric molecules. Recently Lyons (2001) has computed, using a photochemical equilibrium model, the expected mass independent fractionation in NO_X (and HNO_3), OH and ClO species due to such exchange. In this model, the number density profiles of O-containing short lived and

long-lived radicals were computed by balancing total chemical production and loss for each species at a given altitude. The predicted $\Delta^{17}O$ in HNO_3 is about 22 ‰, which agrees well with the observed 23 ‰ in the nitrates from tropospheric aerosols (Michalski and Thiemens, 2000). This model also predicts mass independent fractionation in stratospheric OH with a wide range of value (~ 2 to 45 ‰). Some of these predictions about the transfer of mass independent signature from ozone to other oxygen containing radicals can be tested in the laboratory in future. Such studies will not only constrain the model but also offer an opportunity for better understanding of the atmospheric isotope chemistry.